

COMING CLOSER TO HIGH FREQUENCY GRAVITATIONAL WAVE DETECTION WITH MAGO

Giovanni Marconato^{1,†}, Julien Branlard³, Lukasz Butkowski³, Vijay Chouhan², Can Dokuyucu³, Mona Eberenz¹, Lars Fischer¹, Bianca Giaccone², Ivan Gonin², Anna Grassellino², Martin Hierholzer³, Wolfgang Hillert¹, Matthias Hoffmann³, Timergali Khabiboulline², Tom Krokotsch¹, Alex Melnychuk², Gudrid Moortgat-Pick¹, Andrea Muhs³, Alex Netepenko², Yuriy Orlov², Krisztian Peters³, Sam Posen², Oleg Pronitchev², Marc Wenskat^{1,3}

¹ University of Hamburg, Hamburg, Germany

² Fermi National Accelerator Laboratory FNAL, Batavia, IL, USA

³ Deutsches Elektronen-Synchrotron DESY, Hamburg, Germany

Abstract

In the last years, low frequency gravitational waves (GWs) have been consistently measured by the LIGO-Virgo collaboration, but little to no attention has been paid to higher frequencies GWs in the range of 10 kHz to 100 MHz, at which confirmation for current theories or even new physics could be hidden.

The MAGO 2.0 project aims at filling this gap in the parameter space using superconducting radio-frequency (SRF) cavities. Exploiting the excellent Q-factors of these resonators, we plan to detect tiny harmonic deformations induced by GWs which change the boundary conditions of the oscillating electromagnetic field.

We present the results of the first cold tests ran at DESY and FNAL using the cavity prototype built 20 years ago at the end of the MAGO collaboration, characterizing the RF spectrum, Q-factor and surface resistance. Additionally we introduce the mechanical vibration spectrum characterization and the RF response of the cavity with the injection of a “fake GW” signal using piezoelectric actuators.

INTRODUCTION

Superconducting resonant cavities are a well-established technology in particle accelerator physics, but in the last decade their range of applications has greatly broadened going from dark matter search [1-4] to quantum computing [5-6]. The very high quality factor that these tools offer can be leveraged also in the search for gravitational waves (GWs) in frequency ranges not yet explored by “standard” instruments like for example the earth-based interferometers in the LIGO-VIRGO-KAGRA (LVK) collaboration. Stemming from an idea proposed in the 1970s by Pegoraro *et al.* [7] and Caves [8] the MAGO proposal [9] in the end of 1990s aimed at using SRF cavities to detect gravitational waves in the lower kHz range, since the interferometers had not been built yet. The same concept can be applied to the detection of high frequency GWs in the kHz to MHz, range, where only a small part of the parameter spaces has been covered. This range of frequencies is very interesting because of the absence of known astrophysical sources of GWs, creating an ideal background-free search. Possible sources include primordial

black hole mergers (PBH), one of the candidates for dark matter, and superradiance, another exotic phenomenon that would hint at the presence of bosonic dark matter [10].

Detection Principle

The MAGO proposal uses the so-called heterodyne detection principle: the cavity is designed to have two nearly degenerate EM eigenmodes of which only the lower frequency one (0 mode) is loaded with RF power, while the higher frequency one (π mode) is used as detection mode. The interaction of a GW with the cavity’s walls (mechanical interaction[11]) or the EM field in the cavity itself (Gertsenshtein effect[12]) can cause an upconversion of the RF power at a frequency equal to the sum of the 0 mode frequency plus the GW frequency.

$$\omega = \omega_0 + \omega_{GW} \quad (1)$$

The Gertsenshtein effect becomes only relevant in the GHz frequency range for the GW, therefore in this study we will disregard it. The upconversion condition is resonantly enhanced when the resulting frequency coincides with the π mode frequency, resulting in an enhanced sensitivity. This does not mean that the device would be sensitive only on resonance, as it is possible to broaden the read out sensitivity by strongly overcoupling to the cavity [13].

The coupling of a GW to the superconducting cavity’s walls can be expressed as [14]:

$$\Gamma_+^l := V_{cav}^{-1/3} \cdot M_{cav}^{-1} \int_{V_{cav}} d^3x \rho(\vec{r}) \left(x \xi_{l,x}(\vec{r}) - y \xi_{l,y}(\vec{r}) \right) \quad (2)$$

$$\Gamma_\times^l := V_{cav}^{-1/3} \cdot M_{cav}^{-1} \int_{V_{cav}} d^3x \rho(\vec{r}) \left(x \xi_{l,y}(\vec{r}) - y \xi_{l,x}(\vec{r}) \right) \quad (3)$$

with $+, \times$ two polarizations of the GW, V_{cav}, M_{cav}, ρ respectively volume, mass and density of the cavity and $\xi_{l,x}$ displacement of the l mechanical eigenmode in the x direction. The second step of coupling between mechanical vibration and EM eigen modes can be then described by the following coupling coefficient:

$$C_0^l = \frac{V_{cav}^{1/3}}{2\sqrt{U_0 U_1}} \int_{\partial V_{cav}} d\vec{S} \cdot \vec{\xi}_l(\vec{r}) \left[\frac{1}{\mu_0} \vec{B}_0(\vec{r}) \vec{B}_1(\vec{r}) - \epsilon_0 \vec{E}_0(\vec{r}) \vec{E}_1(\vec{r}) \right] \quad (4)$$

with U_0, U_1 energy stored in both modes, $\vec{B}_{0,1}, \vec{E}_{0,1}$ magnetic and electric field distribution respectively in each

[†] giovanni.marconato@desy.de

mode. As can be seen from Eqs. 2-4 the displacement map of the mechanical eigenmodes and the shape of the EM field in both EM modes is necessary to compute the sensitivity to any GW. Moreover the overlap between GWs frequency and mechanical eigenmode frequency also resonantly enhances the signal. The various eigenmode shapes and frequencies can be obtained using simulation softwares like COMSOL. While the EM eigenmodes are relatively easy to simulate, the mechanical eigenmodes depend heavily on any external component touching the system and even small imperfections that do not affect the EM modes (i.e. vacuum line connection, sustaining frame, small wall deformations) would modify the eigenmodes' spectrum, making simulations difficult and unreliable.

We found that the most reliable way to experimentally determine the mechanical behavior of the MAGO cavity inside its frame might be the use of piezoelectric crystals both as stimulus and as sensors for the walls' displacement, placed in some strategic points determined by a rough simulation of the cavity alone.

MAGO Cavity Prototype

At the end of the MAGO project a third prototype was fabricated but never tested. This prototype consists of a bulk niobium cavity with two quasi-spherical cells and a smaller middle cell intended to be a coupling cell (Fig. 1).

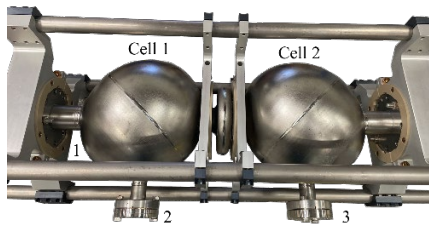


Figure 1: MAGO prototype cavity in its sustaining frame. The numbers show the currently installed antenna position.

The project has been revived by a University of Hamburg – Deutsches Elektronen-Synchrotron (DESY) – Superconducting Quantum Materials and Systems Center at Fermi National Accelerator Laboratory (SQMS-FNAL) collaboration that took over the prototype and is currently further advancing the initial idea.

Before any test, the cavity had to be tuned, due to some deformation along the main axis that occurred while the prototype was stored for more than 20 years. The tuning procedure and results are described in [14] together with the room temperature EM and mechanical characterization.

The results of previous COMSOL simulations (Fig. 2) show the field profiles of the two modes of interest. The shape of the modes is the same in both cells, with the only exception of a π phase shift between the cells in the π mode. This phase difference can be leveraged to selectively suppress one of the modes both in the readout scheme by combining the output signal from the two cells of the cavity or in the input by driving both cells at the same time. This idea was proposed and tested on a different pillbox cavity in the 90s by the PACO collaboration, where they reached a

140dB suppression of the 0 mode in the readout [15]. It is important to remember that in the heterodyne detection, high power is supplied in the 0 mode and an extremely weak signal is expected in the π mode, so it is mandatory to be able to reject as much as possible the 0 mode signal in the readout. These two modes having the same field distribution guarantee a great overlap and therefore increase the coupling coefficient in Eq. 4. Moreover controlling the cell-to-cell distance it is possible to control the coupling and consequently the mode's frequency difference.

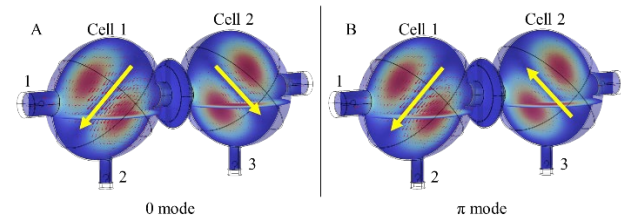


Figure 2: Simulation of the 0 mode (A) and π mode (B) of the MAGO prototype. The colour scale shows the electric field distribution while the arrows represent the magnetic field distribution. The numbering indicates the currently installed antenna position.

RF CHARACTERIZATION

At the moment the cavity has been assembled with three of the four available antennas mounted. The position and labeling of the antennas are shown in Figs. 1 and 2.

Cold Test at FNAL

The first cold test has been carried out by SQMS at FNAL. This test was the first cold characterization of the MAGO prototype since its fabrication more than 20 years ago. The preparation of the cavity is described in [14, 16]. The first important result is shown in the S21 and S31 spectra in Fig. 3, reporting the presence of the two desired modes at frequencies around 2.099750 GHz, at a distance of ~ 11 kHz from each other. The presence of an antiresonance peak in the S21 parameter was predicted by equivalent circuit calculations of the system [14]. This peak corresponds to the eigenfrequency of cell 2 if it wasn't a coupled system. As expected from the equivalent circuit derivation, the antiresonance peak is not visible in the S31 parameter spectrum. The frequency value difference for each eigenmode measured at FNAL or DESY brings only a negligible correction in the sensitivity calculations, since it is on the order of kHz compared with an absolute value of GHz. The difference in signal intensity between the two sets of measurements is given by the different setups: the FNAL measurements were taken using -5 dBm input power and +40 dB amplification in the input line while DESY measurements were taken using 0 dBm input power and +20 dB amplification only on the readout line. Moreover the IF bandwidth used is also different giving a much longer sweeping time for the FNAL measurement. The smaller peaks that appear in these spectra could be due to the frequency jitter of the main peaks over the data acquisition time. The slight difference in the two modes' spacings is also due to this jitter.

The measurement of quality factor vs stored energy inside the cavity gave a maximum stored energy before quenching of 1.3 J at 2 K with a quality factor of $1 \cdot 10^{10}$.

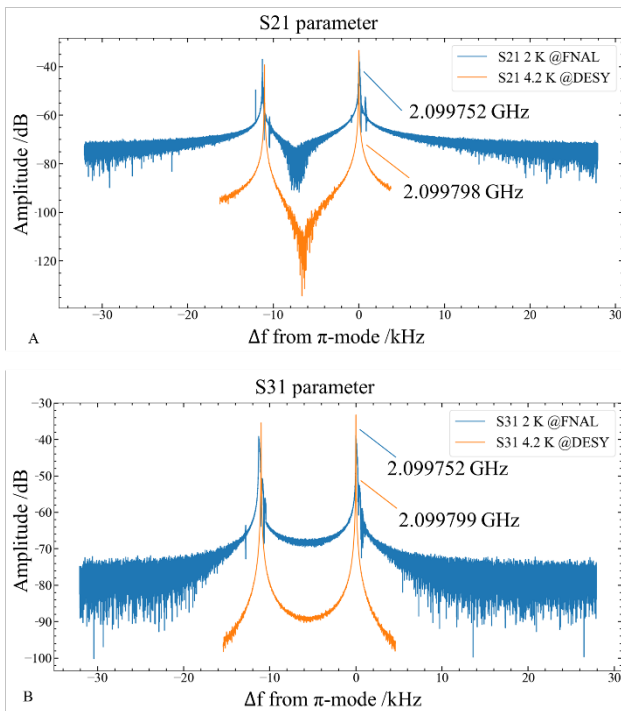


Figure 3: (A) S21 parameter spectrum of the MAGO prototype measured at FNAL at 2 K (blue line) and at DESY at 4.2 K (orange line). Both spectra are centered around the π mode peak frequency, which for the FNAL measurement is 2.099752 GHz, while for the DESY measurement is 2.099798 GHz. (B) S31 parameter spectrum of the MAGO prototype measured at FNAL at 2 K (blue line) and at DESY at 4.2 K (orange line). Both spectra are centered around the π mode peak frequency, which for the FNAL measurement is 2.099752 GHz, while for the DESY measurement is 2.099799 GHz. All FNAL measurements have been taken using -5 dBm input power and +40 dB amplification on the input line, while all DESY measurements were taken with 0 dBm input power and +20 dB amplification on the readout line.

Cold Test at DESY

The same results for the S parameters from the cold test at FNAL have been confirmed at DESY during the second cold test at 4.2 K and are shown in Fig. 3.

The frequency difference between the modes registered at DESY and at FNAL is due to the difference in temperature and pressure in the cryostat and is within expectations. It is instead very important to notice the spacing between the modes remaining constant within measurement uncertainties.

The DESY cold test was conducted only at the temperature of 4.2 K as a preparatory test to develop the low level RF system in preparation for the following 2 K test to take place later this year. In this test a rudimentary version of the PACO detection scheme was implemented only on the readout side, using commonly available phase shifters,

attenuators and combiners, achieving a 50 dB selective suppression of one mode (Fig. 4). Leveraging on the π phase shift between 0 and π mode in cell 2, the output of the two cells was combined introducing a phase shifter on one line as well. With this setup it was possible to selectively suppress the 0 or π mode just by changing the phase shift on the line. The spectrum should be compared with the S31 spectrum in Fig. 3B. This measurement showed us the many technical difficulties in implementing such a scheme. Operating the phase shifters and attenuators manually required extreme precision even for a rough setup like the one we used and the stability over time was in the order of minutes. Achieving higher suppression while minimizing the added noise from the components will be a considerable challenge. Moreover, automation of the controls appears to be mandatory to keep the suppression stable during the whole measurement time, which for a future GW detection run will be much greater than minutes. The full RF scheme is currently being greatly revised from the original MAGO proposal, with the notable addition of the Carrier Suppression Interferometry (CSI) [17] in the readout.

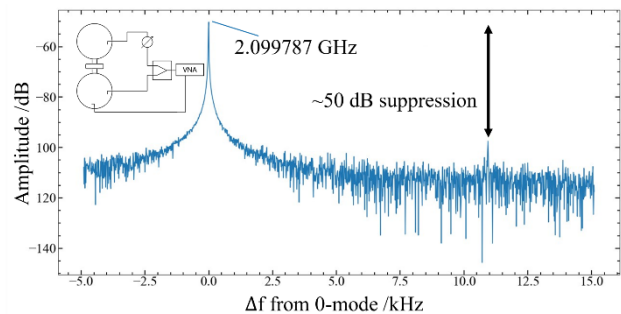


Figure 4: S parameter combining the output of antenna 2 and 3. The simplified RF scheme is shown in the upper left corner. The data is centered around the 0 mode peak at 2.099787 GHz, since the π mode is suppressed. The maximum achieved suppression is about 50 dB.

MECHANICAL CHARACTERIZATION

Before measuring directly on the MAGO prototype we decided to test the mechanical characterization on an easier more controlled, table-top system consisting of a steel sphere of diameter 20 cm and wall thickness 2 mm suspended by three screws on an optical bench. The sphere has first been simulated using COMSOL and then the results have been compared with the experimentally obtained values. The measurement of the vibrations has been carried out using an Attocube FPS 3010 laser interferometer. The piezoelectric crystal PI-PICMA P-882.91 was chosen as excitation source because of some previous experience of the group working with this model and its availability on the market. The piezo has been connected to a waveform generator and kept slightly pressed against the sphere surface on one side, while the laser interferometer was placed on the opposite side pointing at a piece of silicon wafer attached to the sphere surface to enhance the reflectivity (Fig. 5).

Each point in the following plots that show vibrational results has been taken by averaging over one minute of

measurement and the error has been taken as the standard deviation.

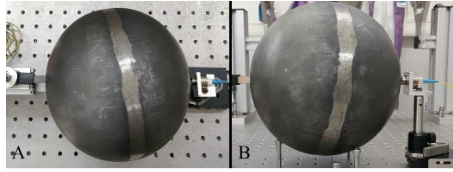


Figure 5: Pictures of the vibrational measurements setup from above (A) and the side (B). The piezo electric crystal is visible on the left side of the sphere and on the right side the end of the optical fiber connected to the laser interferometer.

Piezoelectric Crystal Calibration

The final goal of the study is to understand vibrational eigenmodes in the range of frequencies of interest for GW detection therefore from kHz to MHz. In this study we focused on a smaller range between 1 and 10 kHz.

The elongation of piezo crystals with an applied AC voltage is known to be quasi-linear with the voltage amplitude and non-linear in frequency. Therefore some measurements were performed with the laser interferometer pointing directly on the tip of the piezoelectric crystal in order to determine the expected elongation of the piezo without any load.

The results of the calibrations are shown in Fig. 6. As expected, the linear behavior has been observed in all the relevant applied voltage range for frequencies of 1 kHz and 10 kHz which are the extremes of our analysis.

The results obtained for low frequencies, below 1 kHz, are highly affected by ambient noise we could not suppress with the simple setup we prepared. This is not a major problem given the range of interest but will be addressed in future developments.

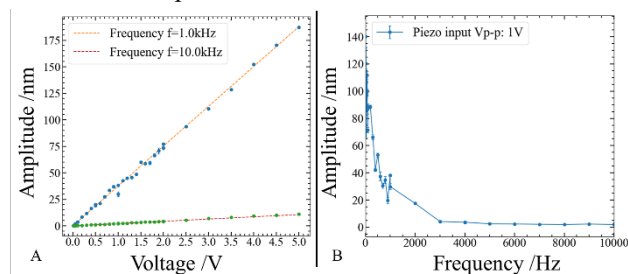


Figure 6: (A) Amplitude of vibration at the selected frequency of the piezoelectric crystal vs applied voltage for 1 kHz (blue dots, orange line) and 10 kHz (green dots and red line). (B) Amplitude of vibration of the piezoelectric crystal vs frequency at fixed voltage of 1 V.

Sphere Characterization

Multiple voltage amplitudes have been tested to determine a good signal to noise ratio while avoiding excessive deterioration of the piezoelectric crystal by applying high force for a prolonged time. In the end a voltage of 1 V was chosen and some relevant frequency ranges were scanned more finely. The ranges of interests were determined by looking at the simulation results. Each measurement has

been normalized by dividing for the piezo expected elongation at the same voltage and frequency measured previously in the calibration. The results show the calculated amplitude ratio between sphere vibration and free piezo excitation in Fig. 7.

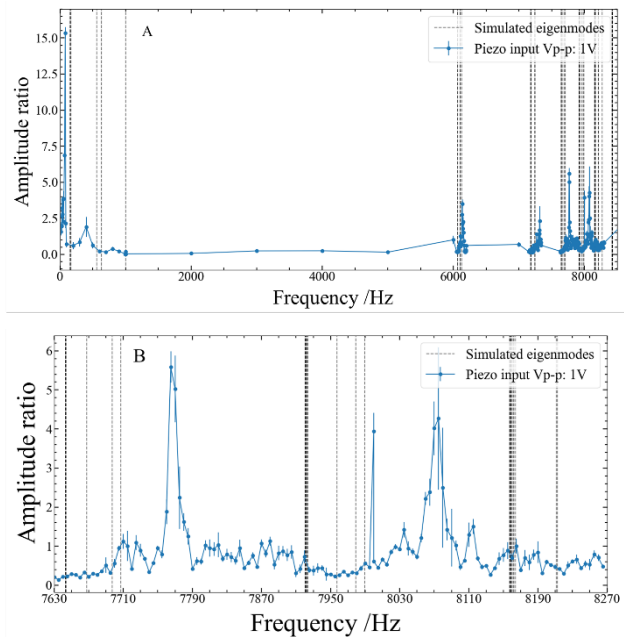


Figure 7: (A) Amplitude ratio of the vibrational measurements on the steel sphere with respect to the free piezo. All measurements were taken with applied voltage to the piezo of 1 V peak to peak. The dashed lines represent the simulated eigenmodes. (B) Particulars of the amplitude ratio measurements on the steel sphere at 1 V_{p-p} excitation in the frequency range from 7.6 kHz to 8.3 kHz.

The presence of resonance modes in the ranges corresponding to some eigenmodes of the system was verified, even though a clear mismatch with the simulation results is present (Fig. 7B). The frequency difference between simulated and measured values is in the order of 5%, giving a good agreement within expected uncertainties. The mismatch can be caused by the uncertainty on the wall thickness which can easily shift the eigenfrequencies. The non-uniformity of the thickness of the wall and the presence of the welding on the sphere equator can also be causes of an eigenmode being distorted and shifted in unpredictable ways. These geometrical uncertainties do not allow us to precisely assign each simulated eigenmode to the measured resonances.

These results show that a characterization of the mechanical eigenmodes using piezoelectric crystals can be obtained, choosing the range of frequencies to precisely scan with the use of simulations.

The next step will be the measurement of the mechanical eigenmodes of the MAGO prototype with an improved setup. This will allow to estimate also the mechanical quality factor of the cavity, a parameter that has only been assumed to be in a plausible order of magnitude of 10^6 in all studies so far [18].

CONCLUSION

The search for high frequency gravitational waves in the range of kHz to MHz using SRF cavities is very promising and might open the path to new discoveries and possibly new physics.

In this manuscript the first RF characterization of the MAGO two-cell prototype has been shown, comparing results from two cold tests carried out at FNAL and DESY. The test showed the intended degenerate TE011 mode with the frequency spacing as expected. The detection scheme has also been tested and proved to be efficient so far. More improvements to the full low level RF system are currently being studied in order to minimize the noise introduced in the system and to maximize the sensitivity to signals appearing in the π mode. The prototype showed a maximum stored energy of 1.3 J and a quality factor of $1 \cdot 10^{10}$ at 2 K.

A proof of principle of the mechanical eigenmodes characterization has been also carried out on a smaller, less complex system, showing the capability to accurately measure mechanical eigenfrequencies, one of the crucial parameters in the GWs sensitivity calculation. With more detailed measurements it will also be possible to characterize the mechanical quality factor of the system at cold, by conducting measurements in liquid helium with the piezoelectric crystals.

Mechanical eigenmode measurements of the real MAGO prototype will be carried out soon, with an improved setup including better insulation from low-frequency noise and finer frequency resolution.

ACKNOWLEDGMENTS

For the loan of the PACO-2GHz-variable cavity, we thank the Istituto Nazionale di Fisica Nucleare, Italy. The authors thank Artur Heck, Ralph Doehrmann, Patrik Wiljes and Marco Voige for their support and useful discussions. This material is based upon work supported by the U.S. Department of Energy, Office of Science, National Quantum Information Science Research Centers, Superconducting Quantum Materials and Systems Center (SQMS) under contract number DEAC02-07CH11359. LF, WH, TK, GM-P, KP and MW acknowledge support by the BMBF under the research grant 05H21GURB2 and the project is also funded/acknowledges support by the Deutsche Forschungsgemeinschaft (DFG, German Research Foundation) under Germanys Excellence Strategy - EXC 2121 ‘Quantum Universe’ – 390833306.

REFERENCES

- [1] A. Romanenko *et al.*, “Search for Dark Photons with Superconducting Radio Frequency Cavities,” *Phys. Rev. Lett.*, vol. 130, no. 26, p. 261801, Jun. 2023. doi:10.1103/PhysRevLett.130.261801
- [2] SHANHE Collaboration *et al.*, “First Scan Search for Dark Photon Dark Matter with a Tunable Superconducting Radio-Frequency Cavity,” *Phys. Rev. Lett.*, vol. 133, no. 2, p. 021005, Jul. 2024. doi:10.1103/PhysRevLett.133.021005
- [3] A. Berlin *et al.*, “Searches for New Particles, Dark Matter, and Gravitational Waves with SRF Cavities,” Mar. 23, 2022, *arXiv: arXiv:2203.12714*. doi:10.48550/arXiv.2203.12714
- [4] R. Cervantes *et al.*, “Deepest sensitivity to wavelike dark photon dark matter with superconducting radio frequency cavities,” *Phys. Rev. D*, vol. 110, no. 4, p. 043022, Aug. 2024. doi:10.1103/PhysRevD.110.043022
- [5] G. Marconato, “Superconducting resonant cavities design and material development for quantum computing and quantum sensing applications,” Master’s Thesis, University of Padova, Padova, Italy, 2025.
- [6] T. Roy, T. Kim, A. Romanenko, and A. Grassellino, “Qudit-based quantum computing with SRF cavities at Fermilab,” in *PoS*, Fermi National Laboratories, Jan. 2024. doi:10.22323/1.453.0127
- [7] F. Pegoraro, E. Picasso, P. Bernard, and L. A. Radicati, “Electromagnetic detector for gravitational waves,” *Phys. Lett. A*, vol. 68, pp. 165–168, Oct. 1978. doi:10.1016/0375-9601(78)90792-2
- [8] C. M. Caves, “Microwave cavity gravitational radiation detectors,” *Phys. Lett. B*, vol. 80, no. 3, pp. 323–326, Jan. 1979. doi:10.1016/0370-2693(79)90227-2
- [9] R. Ballantini *et al.*, “Microwave apparatus for gravitational waves observation,” Feb. 11, 2005, *arXiv: arXiv:gr-qc/0502054*. doi:10.48550/arXiv.gr-qc/0502054
- [10] N. Aggarwal *et al.*, “Challenges and Opportunities of Gravitational Wave Searches above 10 kHz,” Jan. 20, 2025, *arXiv: arXiv:2501.11723*. doi:10.48550/arXiv.2501.11723
- [11] L. Fischer, “Optimization of SRF Cavities for High-Frequency Gravitational Wave Detection,” Master’s Thesis, University of Hamburg, Hamburg, Germany, 2024.
- [12] M. E. Gertsenshtein, “Wave resonance of light and gravitational waves,” *Soviet Phys JETP*, vol. 14, p. 84, Jan. 1962.
- [13] A. Berlin *et al.*, “Electromagnetic cavities as mechanical bars for gravitational waves,” *Phys. Rev. D*, vol. 108, no. 8, p. 084058, Oct. 2023. doi:10.1103/PhysRevD.108.084058
- [14] L. Fischer *et al.*, “First characterisation of the MAGO cavity, a superconducting RF detector for kHz–MHz gravitational waves,” *Class. Quantum Gravity*, vol. 42, no. 11, p. 115015, May 2025. doi:10.1088/1361-6382/add8da
- [15] P. Bernard, G. Gemme, R. Parodi, and E. Picasso, “A detector of small harmonic displacements based on two coupled microwave cavities,” *Rev. Sci. Instrum.*, vol. 72, no. 5, pp. 2428–2437, May 2001. doi:10.1063/1.1366636
- [16] M. Wenskat and B. Giaccone, “Detection of high-f Gravitational Waves using SRF Cavities,” presented at the 22nd International Conference on RF Superconductivity (SRF’25), Tokyo, Japan, Sep. 2025, paper FRB05, this conference.
- [17] L. Springer *et al.*, “Phase Noise Measurements for L-Band Applications at Attosecond Resolution,” *IEEE Trans. Instrum. Meas.*, vol. 71, pp. 1–7, 2022. doi:10.1109/TIM.2022.3170975
- [18] R. Ballantini *et al.*, “Experimental Results on SCRF Cavity Prototypes for Gravitational Wave Detection,” in *Proc. SRF’03*, Lübeck, Germany, Sep. 2003, paper MOP31, pp. 106–110.